REMARKS

Claims 1 and 9 have been amended to clarify the invention. Support for the amendments to Claim 1 can be found in paragraphs 0012 (for nematic phase) and 0047 (for cooling step) of the substitute specification previously submitted, for example. Support for the amendments to Claim 9 can be found in paragraphs 0019 (for nematic phase) and 0047-0048 (for cooling step and irradiating step) of the substitute specification previously submitted, for example. Claims 18 and 19 have been added. Support for Claims 18 and 19 can be found in paragraph 0046 of the substitute specification previously submitted, for example. Claims 14-17 have been withdrawn from consideration as being directed to a non-elected species. If generic claims are allowed, rejoinder of Claims 14-17 is respectfully requested.

The amendments do not raise the addition of new matter to the application. Applicant respectfully requests entry of the amendments and reconsideration of the application in view of the amendments and the following remarks.

Rejection of Claims 9 and 10 Under 35 U.S.C. § 112

Claims 9 and 10 have been rejected under 35 U.S.C. § 112, second paragraph, with regard to the indefinite term set forth in the office action. The Examiner asserts that it is unclear how the alignment is fixed. In Claim 9, the phrase "cooling the aligned liquid crystalline composition to a temperature lower than a glass transition temperature of the liquid crystal polymer" has been introduced to make the indefinite term clear, thereby obviating the rejection. Thus, Applicant respectfully requests withdrawal of the rejection.

Rejection of Claims 1, 2, 9 and 10 Under 35 U.S.C. § 102

Claims 1, 2, 9 and 10 have been rejected under 35 U.S.C. § 102(b) as being anticipated by US 5,620,781 (Akashi et al.). Applicant respectfully traverses this rejection.

The Examiner asserts that Akashi et al. discloses in paragraph bridging cols. 30-31 that after the substrate is coated with the liquid crystal polymer which is in a liquid crystal state, homeotropically aligning the liquid crystal polymer by heating. However, contrary to the Examiner's assertion, Akashi et al. discloses in the same parts: "when the medium is imagewise heated by means of a thermal head or a laser beam to become isotropic and then rapidly quenched, the heated part is fixed in the isotropic state to constitute a transparent recorded part."

8

(Emphasis added) That is, Akashi et al. discloses "isotropic" not "homeotropic." Homeotropic requires perpendicular (See Fazio et al., page 3 as enclosed herewith). Isotropic just means all same. Fazio et al., page 11 shows the homeotropic to isotropic phase transition.

On the other hand, Akashi et al. discloses that suitable <u>orientating films</u> (8) include those for homogeneous orientations, but <u>never</u> discloses that <u>liquid crystal polymer layer</u> (3) is homeotropically aligned (see column 30, lines 31-32).

Further, the Examiner asserts that Akashi et al. discloses in col. 30, lines 52-53 that a substrate on which a vertical alignment film is not formed. However, contrary to the Examiner's assertion, Akashi et al. discloses in the same parts: "it is the simplest system, requiring no orientation of the liquid crystal molecules." This means that in Akashi et al., the liquid crystal molecules can be used <u>without orientation</u> and therefore this disclosure in Akashi is irrelevant to the present invention which <u>requires homeotropic alignment</u>. Akashi et al. does not disclose homeotropically aligning the liquid crystal polymer on a substrate on which a vertical alignment film is not formed.
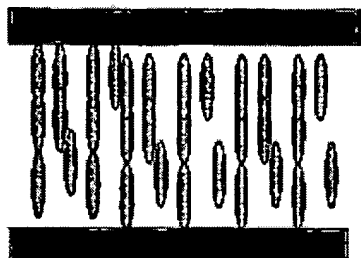
Accordingly, Akashi et al. fails to disclose every element of the claimed invention, and withdrawal of the rejection under 35 U.S.C. §102 is respectfully requested.

Rejection of Claims 1, 2, 9 and 10 Under 35 U.S.C. § 102
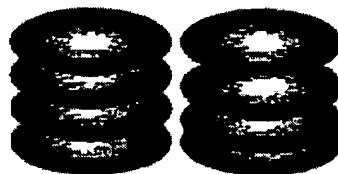
Claims 1, 2, 9 and 10 have been rejected under 35 U.S.C. § 102(b) as being anticipated by US 5,730,900 (Kawata). Applicant respectfully traverses this rejection.

Claim 1 as amended herein recites: heating the liquid crystal polymer to form a homeotropically-aligned liquid crystal polymer which shows <u>nematic</u> phase. Nematic liquid crystals are liquids of <u>rodlike</u> molecules displaying a long-range orientational order (see page 1, right column of Golestanian et al. as enclosed herewith). That is, the homeotropically-aligned liquid crystal polymer of the present invention is <u>rod-like</u> liquid crystals, whereas discotic liquid crystals of Kawata are <u>disc-like</u> liquid crystals as shown in the below figures. In addition, "nematic" is entirely different from "discotic nematic" which requires <u>no</u> long-range order (see Kumar, page 199 as enclosed herewith). At least for this reason, Claim 1 is distinct from Kawata.

Nematic (Rod-like shape)   Discotic (Disc-like shape)

Homeotropic alignment

Further, although Kawada discloses a mixture of a liquid crystalline polymer and nonliquid-crystalline polymer (see column 31, line 67), Kawata does not disclose the specific liquid crystal polymer recited in Claim 1. The side chain type liquid crystal polymer used in the present invention is a polymer **of** a monomer unit (a) containing a liquid crystalline fragment side chain and a monomer unit (b) containing a non-liquid crystalline fragment side chain. That is, the liquid crystal polymer contains both the monomer unit (a) and the monomer unit (b) <u>in a single molecule</u>, which is entirely different from the mere mixture of a liquid crystalline polymer and a nonliquid-crystalline polymer.

Accordingly, Kawata fails to disclose every element of the claimed invention. Thus, Claim 1 as well as Claims 2, 9 and 10 could not be anticipated by Kawata. It is respectfully requested that the rejection under 35 U.S.C. § 102(b) be withdrawn.

Rejection of Claims 1, 2, 9 and 10 Under 35 U.S.C. § 102

Claims 1, 2, 9 and 10 have been rejected under 35 U.S.C. § 102(e) as being anticipated by US 6,379,758 (Hanmer et al.). The claims as amended herein could not be anticipated by Hanmer et al. as explained below.

The liquid crystal polymer used in the present invention is homeotropically aligned on a substrate on which a vertical alignment film is not formed because the liquid crystal polymer contains both the monomer unit (a) and the monomer unit (b) <u>in a single molecule</u>. The

10

monomer unit (a) is also homeotropically aligned by action of the monomer unit (a) presented in the same molecule.

Hanmer et al. fails to disclose the above significant feature. In Hanmer et al., even if a first monomer corresponding to the monomer unit (a) and a second monomer corresponding to the monomer unit (b) are used, they should be used in admixture since these monomers do not exist in a single molecule. Therefore, a homeotropically-aligned polymer can not be obtained from the first monomer and the second monomer on a substrate on which a vertical alignment film is not formed.

The Examiner points out that there exists no limitation in the instant claims requiring the liquid crystal polymer to be a polymer before applying it to the substrate. In response to the Examiner's assertion, Claims 1 and 9 have been amended to recite "said liquid crystal polymer being a polymer prior to the coating thereof and being capable of homeotropic alignment by heating."

According to the claimed invention, some advantages can be obtained by using liquid crystal polymer instead of liquid crystal monomers. Since a liquid crystal polymer used in Claim 1 does not have any reactive groups, stability (no reaction) can be obtained after forming a film. In contrast, a liquid crystal monomer used in Hanmer et al. is not stable since reactive groups remain in a film. Further, if a film formed by a liquid crystal polymer is oriented, the alignment is not easy to be disordered. Furthermore, Hanmer et al. requires irradiating ultraviolet to fix the alignment of liquid crystal monomers, whereas the present invention recited in Claim 1 does not require it due to using a liquid crystal polymer, thereby decreasing the number of manufacturing processes.

Accordingly, the processes disclosed in Hanmer et al. are entirely different from the present invention. Hanmer et al. fails to disclose every element of the claimed invention, and withdrawal of the rejection under 35 U.S.C. § 102(e) is respectfully requested.

CONCLUSION

In light of the foregoing, it is respectfully submitted that the present application is in condition for allowance. Should the Examiner have any remaining concerns which might prevent the prompt allowance of the application, the Examiner is respectfully invited to contact the undersigned at the telephone number appearing below.

Please charge any additional fees, including any fees for additional extension of time, or credit overpayment to Deposit Account No. 11-1410.

Respectfully submitted,

KNOBBE, MARTENS, OLSON & BEAR, LLP

Dated: _____October 12, 2004_____ By: _____

Daniel E. Altman
Registration No. 34,115
Attorney of Record
Customer No. 20,995
(949) 760-0404

H:\DOCS\TOS\UNIU42.001AUS\UNIU42.001AUS.AMEND4.DOC
101204

Alignment and alignment dynamics of nematic liquid crystals on Langmuir-Blodgett mono-layers

V. S. U. Fazio, L. Komitov and S. T. Lagerwall

Department of Microelectronics & Nanoscience,
Chalmers University of Technology & Göteborg University,
S-41296 Göteborg, Sweden

Abstract

Mono-layers of stearic and behenic acids deposited with the Langmuir-Blodgett technique, were used as aligning films in nematic liquid crystal cells. During the filling process the liquid crystal adopts a deformed quasi-planar alignment with splay-bend deformation and preferred orientation along the filling direction. This state is metastable and transforms with time into homeotropic once the flow has ceased. The transition is accompanied by formation of disclination lines which nucleate at the edges of the cell. The lifetime of the metastable splay-bend state was found to depend on the cell thickness. On heating, anchoring transition from quasi-homeotropic to degenerate tilted alignment in form of circular domains takes place near the transition to the isotropic phase. The anchoring transition is reversible with a small hysteresis.

1   Introduction

Liquid crystal cells exhibiting uniform orientational alignment over large areas are required in most device applications. The usual techniques used to obtain a preferred orientation, or anchoring direction, relay on inducing physical or chemical interactions between a prepared substrate and the liquid crystal molecules [1]. Among them the Langmuir-Blodgett (LB) technique, which enables the deposition of organic aligning films with controlled molecular order and thickness and very high reproducibility [2,3], is still in a research state but represents a high potential for future display alignment in an industrial scale.

When a substrate has been covered with a LB mono-layer, a possible aligning mechanism for a liquid crystal is that the molecules penetrate into the layer of aliphatic chains. They then adopt the orientation of these chains, which leads to homeotropic or conical anchoring, depending on the chains' orientation [1].

Table 1: Long-chain fatty acid compounds used in this experiment.

Common name	Structure	Abbreviation
stearic	$C_{17}H_{35}COOH$	C18
behenic	$C_{21}H_{43}COOH$	C22

In this work mono-layers of stearic (C18) and behenic (C22) acids were used as aligning layers in nematic liquid crystal (NLC) cells for obtaining a uniform homeotropic surface-induced orientation. [4,5] The alignment was studied during the filling process and pursued during the relaxation to the equilibrium state. The temperature stability of this state was also investigated.

2 Experiment

2.1 Film preparation

Mono-layer formation was achieved by spreading a solution of stearic or behenic acid (see Table 1) on the surface of ultrapure Milli-Q water in a LB trough (KSV 3000) held in a clean room environment to limit contamination of the trough by dust.

The substrate used in the experiments was tin oxide (ITO) coated glass. Glass plates were cut to a size of 75 mm×30 mm and pre-cleaned in an ultrasound bath filled with ultrapure water to eliminate the bigger dust particles and the residues from cutting. They were then cleaned during 8 minutes in an ultrasound bath filled with a mixture of 5 parts of H_2O, 1 part of NH_3, and 1 part of H_2O_2 at a temperature of 80°C. Finally they were rinsed in a three stage cascade with Milli-Q water and again rinsed and dried in a centrifuge. With this procedure we could eliminate both organic and inorganic contaminations. The glass plates were stored in the clean room so that they could last cleaned for at least two weeks.

The stearic and behenic solutions were made to a concentration of 1 mM in Merck chloroform. The sample material was spread on the water surface with a clean, all glass, Hamilton syringe. After a time lapse of ca. 10 minutes to allow the solvent to evaporate, the mono-layer was compressed at a a rate of approximately 0.3×10^{-3} $(nm^2\,s^{-1}molecule^{-1})$ until the requested pressure was reached.

The glass substrates were immersed in the sub-phase before spreading the mono-layer, and the transfer to the glass occurred during the extraction of the glass from the sub-phase at a controlled speed (10 mm/min), keeping the surface pressure constant.
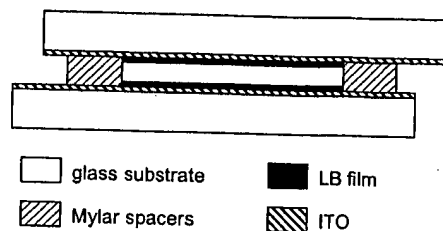
Figure 1: Cross-section of a cell. The ITO layer is in the inner part of the cell with the LB film on top of it. The proportions are symbolic.

2.2 Cell fabrication and observations

Sandwich cells were made with the ITO layers in the inner part (Figure 1) and spaced with polyester of various thickness supplied by Mylar. Care was taken not to touch, and thus contaminate, the inside surface of the cells.

The cells were capillary filled with MBBA (supplied by Aldrich) at room temperature. The observations on them were made with a microscope where the sample is inserted in a hot stage between crossed polarisers. Due to the birefringence of liquid crystals the planar phase, where the molecules lie parallel to the planes of the polarisers, appears very coloured and changes appearance as the sample is rotated. On the other hand, the homeotropic phase, where the long axis of the liquid crystal is oriented perpendicularly to the planes of the polarisers, looks uniformally dark. The microscope was also equipped with a video-camera connected to a computer: it was possible to take pictures of the samples at regular time intervals and then record the evolution of the alignment state.

3 Results

3.1 Isotherms

In Figure 2 the surface pressure versus molecular area isotherms for films of stearic acid (C18) and behenic acid (C22) are shown. Table 2 provides a summary of the three mono-layer phases observed in the isotherms of Figure 2.

Table 2: Condensed mono-layer phases for fatty acids. (After Petty, 1996.)

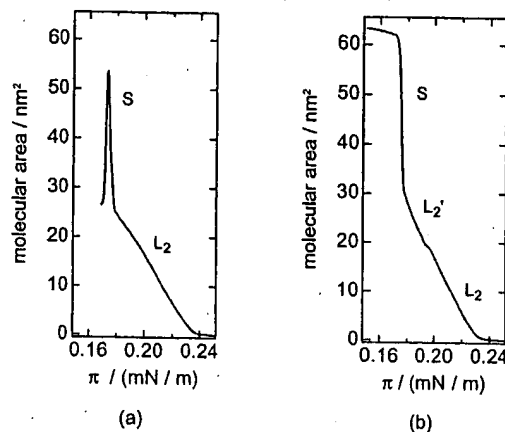| Phase	Name	Characteristics
L_2	liquid-condensed	Slightly tilted molecular chains.
L'_2	liquid-condensed	Tilted chains, but with tilt direction in excess of 45° relative to L_2 phase; similar compressibility as L_2 phase.
S	solid	Upright molecules; less compressible than L_2 and L'_2 phases; high collapse pressure.

Figure 2: (a) Surface pressure versus area per molecule isotherm for stearic acid. We can distinguish the L_2, or liquid-condensed phase [2], and the S or solid phase. (b) Surface pressure versus area per molecule isotherm for behenic acid. In addition to the L_2 and the S phases, here we have a slightly different liquid-condensed phase, the L'_2 phase. See Table 2 for the phase characteristics.

The deposition pressure for the LB films was chosen at 20 mN/m. In this condition we have the liquid-condensed phase of the mono-layer for both compounds (see Figure 2).

3.2 Alignment

The cells were capillary filled with MBBA at room temperature (where MBBA is in the nematic phase). During filling we have the alignment condition in which the orientation of the MBBA molecules is quasi-planar with a preferred alignment along the filling direction: the molecules in the centre of the cell are essentially parallel to the substrate and a splay-bend deformation in the NLC is induced by the presence of the aligning layer [6] (see Figures 3(a) and 3(b)). As soon as the flow stops, because the cell is completely filled with MBBA, domains of homeotropic alignment start to nucleate at the edges of the sample and continuously grow until the whole sample becomes homeotropic.

An example of how the homeotropic domains expand in the cell is given in Figure 4. The line which devides the homeotropic domain from the quasi-planar one is found to be a disclination line of strength $|S| = 1/2$. Such a disclination line should appear bright between crossed polarisers and dark between parallel polarisers (see Figure 5).

A simple scheme of disclination lines of strength $|S| = 1/2$ is depicted in Figure 6. Because of the LB aligning layer the defect moves into the quasi-
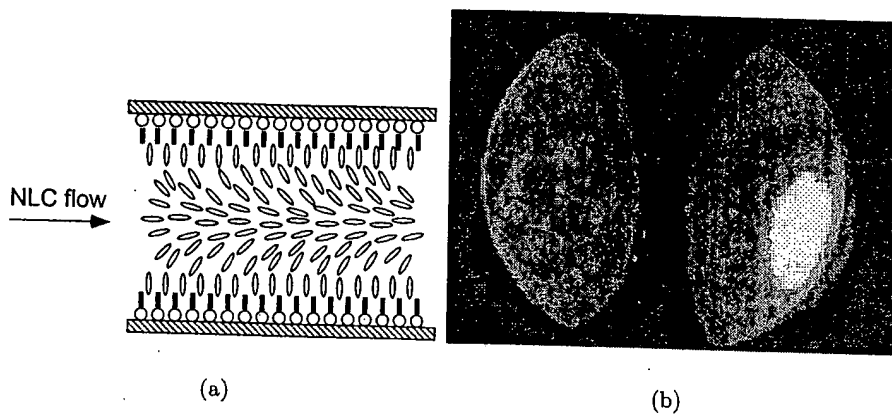
(a)

(b)

Figure 3:   (a) During filling the orientation of the LC molecules is quasi-planar (the molecules lie parallel to the glass substrate) with a preferred alignment along the filling direction. The molecules in the centre of the cell are essentially parallel to the substrate and a splay-bend deformation in the NLC is induced by the presence of the aligning layer [6]. (b) Conoscopic picture of a 22.3 μm thick cell with aligning C18 mono-layer during the NLC filling. The picture shows that the NLC is oriented as depicted in Figure (a) [7]: the molecules in the center of the cell are aligned in the filling direction and a splay-bend structure is induced by the presence of the aligning LB films [8].
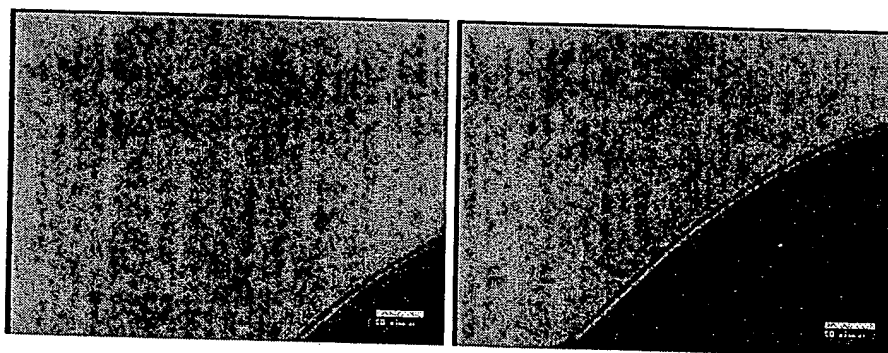

Figure 4:   Cell between crossed polarisers. The LB aligning mono-layer is C18 and the thickness of the cell is 12.5 μm. The cell is completely filled with MBBA, the flow has ceased and the homeotropic domain (dark) expands into the quasi-planar domain (light). The two pictures were taken with a time interval of 30 s.
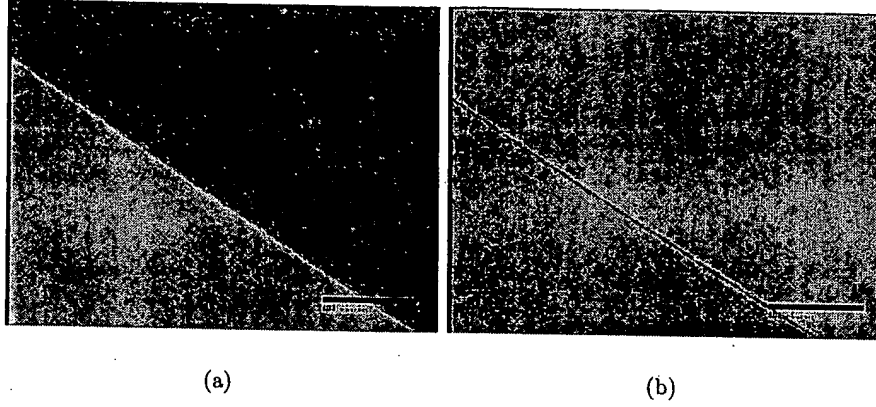
(a)   (b)

Figure 5:   (a) Cell between crossed polarisers. The aligning mono-layer is C18 and the cell thickness is 14.4 μm. The disclination line appears bright. (b) The same cell, a few seconds later, now between parallel polarisers. The disclination line appears dark.
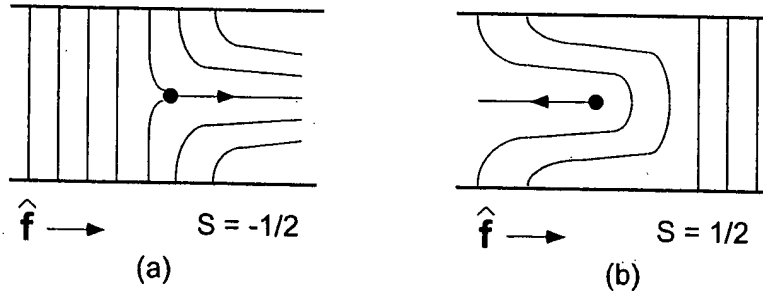

$\hat{f}$ —►   S = -1/2 $\hat{f}$ —►   S = 1/2
        (a)   (b)

Figure 6:   Schematic model of disclinations of strength $|S| = 1/2$. $\hat{f}$ is the filling direction. The parallel vertical lines represent the homeotropically aligned area. The black circles represent the singularities which move into the quasi-planar splay-bend deformed domain. (a) An $S = -1/2$ singularity propagates along the filling direction. (b) An $S = 1/2$ singularity propagates against the filling direction. When two such lines meet, the singularities annihilate (-1/2 + 1/2 =0), leaving a defect-free homeotropic domain.
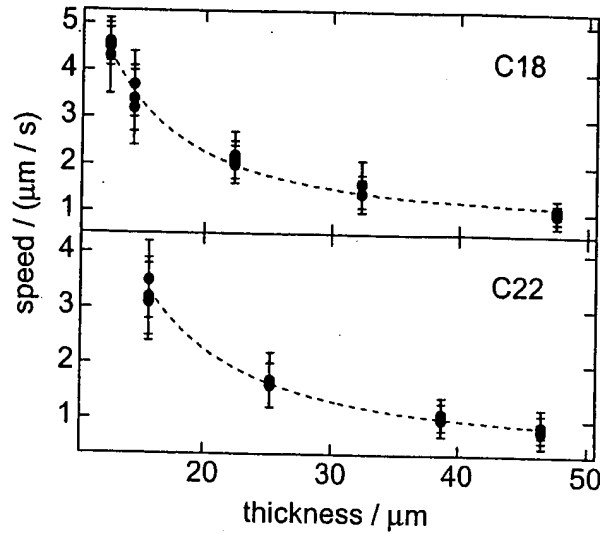
Figure 7: Speed of expansion of the homeotropic domains as a function of the cell thickness, for cells with C18 and C22 as aligning layers. The dots are the experimental values and the dashed lines are fits to the function $a + bL^{-2}$, where a and b are two constants.

planar area, the effect being the expansion of the homeotropic domain.

A priori, we cannot know how much the fatty acid chains are affected by the filling flow. At a solid surface the flow velocity is zero but here it may not be zero in the boundary layer of the chains. Nevertheless we have in Figure 3(a) depicted these chains as being unaffected by the flow and shown them in their homeotropic equilibrium (static) condition. Under this hypothesis, the only driving mechanism behind the propagation of the splay-bend into homeotropic alignment is the elastic distorsion in the liquid crystal.

We measured the speed with which the homeotropic domains expand in the cells by taking pictures at fixed time intervals for several cell thicknesses. The speed was calculated as the area covered by the front of the homeotropic domains in the time interval, divided by the length of the front and the time interval. The results are shown in Figure 7.

For both mono-layer materials Figure 7 shows that the speed of expansion of the homeotropic domains decreases as the cell thickness increases. For cells thinner than $12 \, \mu m$ the speed of expansion of the homeotropic domains is even larger that the actual speed of filling, so that no relaxation process can be observed.

Whereas the propagation speed of the disclination lines depends on the layers thickness, it does not depend on time. It is thus not a diffusive process. This conforms well with our previous hypothesis that the driving

mechanism is the elastic relaxation of the splay-bend deformation in the liquid crystal, because the elastic torque will everywhere be the same behind the propagating front. Its speed will therefore be directly related to the speed of relaxation.

For a small disturbance of amplitude δn and wave vector q we may write the elastic free energy density as

$$\mathcal{F} = \frac{1}{2}Kq^2(\delta n)^2, \tag{1}$$

where K is the characteristic elastic constant. The elastic torque

$$\Gamma = -\frac{\partial \mathcal{F}}{\partial \delta n} = -Kq^2\delta n \tag{2}$$

then gives the dynamic equation

$$\gamma \frac{d\delta n}{dt} + Kq^2\delta n = 0, \tag{3}$$

where γ is the viscosity of the liquid crystal. The characteristic time of relaxation is then

$$\tau = \frac{\gamma}{Kq^2} \sim L^2, \tag{4}$$

where L is the cell thickness. In the present case this relaxation time towards the homeotropic state is proportional to the inverse speed with which the homeotropic domains expand in the quasi-planar domains, thus

$$v \sim L^{-2}. \tag{5}$$

We fitted the experimentally measured speed of expansion of the homeotropic domains to functional relations and found, instead (cfr. Figure 7), a good agreement with

$$v = a + bL^{-2}. \tag{6}$$

As $L \to \infty$, $v \to a$, and we may write

$$v = v_s + bL^{-2}, \tag{7}$$

where v_s is a velocity of the order of $1\,\mu m/s$. As v_s is independent on L we interpret it as characteristic of the surface, coming from a rapid relaxation in the boundary layer of the chains, which propagates the homeotropic state into the liquid crystal bulk. We thus have to conclude that the chains are distorted by the filling flow, but rapidly and forcefully relax to their equilibrium (static) state. In other words, we believe that the LB film itself does have an active rôle in the dynamics of the alignment transition. Therefore Figure 8 probably shows a more correct picture of the surface anchoring than Figure 3(a) which corresponds to our original hypothesis.
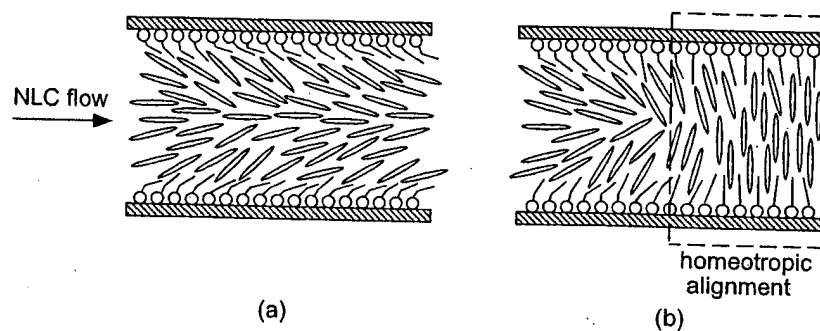
(a)   (b)

Figure 8:   (a) During filling the LB boundary layer seems to be strongly influenced with the chains aligning along the filling direction. (b) When the flow stops the LB film and the splay-bend deformed liquid crystal both contribute to the relaxation towards the homeotropic state.
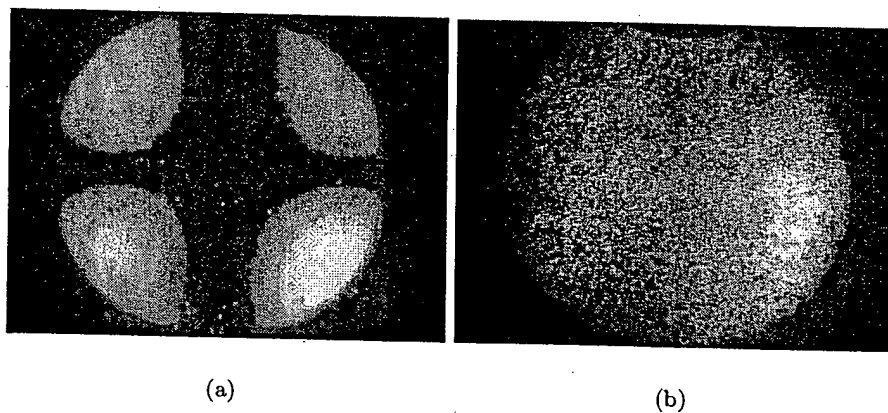

(a)   (b)

Figure 9:   (a) Conoscopic picture of a 14.4 μm thick cell with C18 as aligning layer: a very good homeotropic alignment is achieved. (b) Conoscopic picture of a 15.7 μm thick cell with C22 as aligning layer: the alignment is not homeotropic and not well defined. For both mono-layer materials the alignment is found to be independent on cell thickness.

The homeotropic alignment was studied by conoscopy and the conoscopic pictures of samples with the two aligning layers are shown in Figure 9. As we can see from the figure, a good homeotropic alignment was obtained with C18 as aligning layer and a much less good one with C22 as aligning layer. We believe that the reason for the different anchoring properties should be traced to the behaviour of C18 and C22 at the air-water interface, i.e. in the isotherms of Figure 2. At the deposition pressure of 20 mN/m C18 is in the liquid-condensed L_2 phase, while C22 is in the slightly more condensed liquid-condensed L'_2 phase, where the molecules are strongly tilted with respect to the molecules in the L_2 phase. It is likely that this large tilt of the behenic acid chains causes a large pretilt of the NLC molecules instead of homeotropic alignment.

The alignment was found to be independent on the cell thickness, indicating the main rôle of the mono-layer material.

3.3 Anchoring transition

On heating, we observed a first-order anchoring transition [4] in a very narrow temperature range, just below the clearing point. At the transition a set of bright circular domains with dark crosses appear in the sample; at constant temperature, they grow and colalesce, forming larger domains. The appereance of these domains between crossed polarisers is consistent with a degenerated tilted orientation of the NLC molecules, or conical anchoring, also expected in the case of LB aligning films [1].

On increasing the temperature, the transition to the isotropic phase takes place inside the domains (Figures 10(a) and 10(b)). On cooling from the isotropic phase the bright domains appear again and the transition to the nematic phase takes place inside the domains (Figures 10(c) and 10(d)).

Following Safran et al. [9], we think that the surfactants molecules are arranged in soliton-antisoliton pairs randomly distributed over the substrate area. Depending on the length of the tails and on the temperature, those structures can be large enough to prevent the uniform homeotropic alignment, which may be the case in the C22 mono-layer. If the soliton-antisoliton pairs are not too large, they can give a uniform homeotropic alignment in the bulk. However, they are the germs of the conical structures appearing at the anchoring transition.

4   Conclusions

The surface induced homeotropic alignment in NLC cells by LB mono-layers of stearic and behenic acids has been investigated. Stearic acid was found to be very good for aligning NLC in the homeotropic state, whereas behenic does not give a well defined alignment.
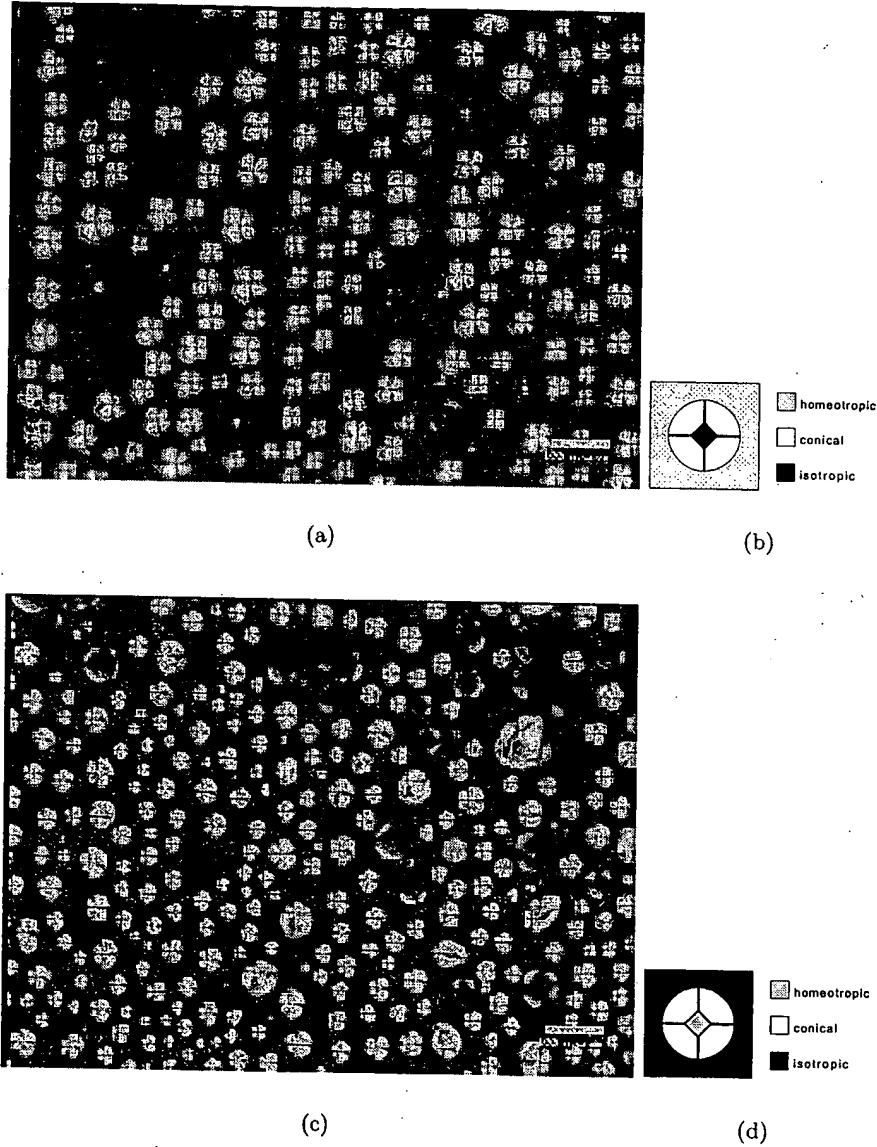
(a)

(b)

(c)

(d)

Figure 10:   (a) Nematic to isotropic phase transition in a cell with C18 as aligning layer. The dark gray background is the homeotropic phase. In the circular domains the alignment is conical. The isotropic phase appears inside the domains. (b) Scheme of the homeotropic to isotropic phase transition. (c) Isotropic to nematic phase transition in the same cell. Now the dark background is the isotropic phase and in the circular domains the alignment is again conical. The homeotropic state appears inside the domains. (d) Scheme of the isotropic to homeotropic phase transition.

[9] S. A. Safran, M. O. Robbins, and S. Garoff. Tilt and splay of surfactants on surfaces. *Phys. Rev. A*, 33(3):2186 –2189, 1986.

Casimir Torques between Anisotropic Boundaries in Nematic Liquid Crystals

Ramin Golestanian[1,2], Armand Ajdari[1], and Jean-Baptiste Fournier[1]

[1]*Laboratoire de Physico-Chimie Théorique, ESA CNRS 7083, E.S.P.C.I., 75231 Paris Cedex 05, France*
[2]*Institute for Advanced Studies in Basic Sciences, Zanjan, 45195-159, Iran*
(July 10, 2004)

Fluctuation-induced interactions between anisotropic objects immersed in a nematic liquid crystal are shown to depend on the relative orientation of these objects. The resulting long-range "Casimir" torques are explicitly calculated for a simple geometry where elastic effects are absent. Our study generalizes previous discussions restricted to the case of isotropic walls, and leads to new proposals for experimental tests of Casimir forces and torques in nematics.

In the last decade, much theoretical attention has been paid to "Casimir" forces in structured complex fluids [1–3]. The pioneering work of Casimir showed that two uncharged conducting plates attract each other in vacuum, due to the modification of the electromagnetic fluctuations imposed by the plates [4]. In complex fluids, similar interactions should exist between embedded objects, as the thermal fluctuations of the medium's elastic distortions are restrained by the boundary conditions imposed by the objects. These interactions are believed to act between bounding surfaces or immersed inclusions in critical fluids or superfluids [5,6], in liquid crystals [7–10], in bilayer membranes [11–13], and also between rodlike polyelectrolytes [14–17]. Nematic liquid crystals are anisotropic fluids with a quadrupolar long-range order. They are considered as good candidates for the direct observation of "Casimir" interactions in complex fluids. However, clear experimental evidences have to date been scarce [2]. This is probably due to the weakness of fluctuation-induced effects when compared to that of permanent elastic distortions, which are often present.

Although nematic liquid crystals are well-known to display orientational effects [18], no "Casimir" interaction directly connected to these orientational properties of nematics have so far been discussed. Here, we demonstrate that thermal fluctuations in nematic liquid crystals can induce *torques* between bounding surfaces [19]. The existence of "Casimir" torques between objects embedded in complex fluids is usually caused by the anisotropy in the *shape* of the objects [12,15,17]; here we report on a more subtle effect occurring between infinite plates with translational symmetry. To emphasize the "Casimir" effect, we focus on a situation in which no average elastic distortion is present: two parallel plates with a surface energy favoring an orientation of the local average molecular alignment (director) *perpendicular* to the surfaces. The ground state is therefore the distorsionless state in which the director is everywhere perpendicular to the boundaries. A "Casimir" torque can arise due to the *anisotropy* in the rigidity of the surface energy: we assume that deviations from the preferred normal surface orientation is easier in one direction than in the orthogonal one. (This property can be experimentally obtained from a grating surface treated for homeotropic anchor-

ing [20], or by depositing on top of a substrate which is conventionally treated to give planar anchoring a very thin layer of a material promoting homeotropic anchoring [21].) In this geometry, we calculate the "Casimir" interaction, and show that it depends not only on the distance between the two plates, but also on their relative orientation. At the end of the paper, we argue that this leads to effects easier to measure than the direct force between the plates.

Nematic liquid crystals are liquids of rodlike molecules displaying a long-range orientational order. The local average molecular axis is represented by a unit vector $\pm\mathbf{n}$, called the "director". The bulk ground state corresponds to a uniform director field and the Frank elasticity describes the free energy associated with gradients of the director [22]. Bounding plates often favor some orientation of the director: this phenomenon is known as *anchoring* [18]. The simplest situations correspond to a preferred orientation normal to the plates (homeotropic anchoring) or parallel to the plates (planar anchoring). Here we employ a path integral method to study the "Casimir" energy of a nematic liquid crystal confined between two parallel plates at a separation d, at which we assume an homeotropic anchoring with anisotropic strength as described above. We calculate the fluctuation-induced interaction between the two plates when the axes of weakest anchoring strength are placed at a relative angle θ (see Fig. 1), and find

$$\mathcal{F}(\theta, d) = -\frac{k_B T}{8\pi d^2} \times \sum_{k=1}^{\infty} \frac{\cos^k 2\theta}{k^3}, \qquad (1)$$

per unit area of the plates. The angle dependence in this interaction shows that the plates experience a long-range fluctuation-induced torque, that decays algebraically as $1/d^2$, and tends to align the directions of weakest rigidity.

We start with the broken symmetry configuration of lowest energy, in which the director field is aligned along the z-axis, and restrict ourselves to small fluctuations $\delta\mathbf{n} = \mathbf{n} - \hat{z}$ of the director around this ground state (see Fig. 1). The bulk cost of such a fluctuation can be described by an effective Hamiltonian

$$\mathcal{H} = \frac{K}{2} \iiint d^3\mathbf{r} \left[\nabla \delta\mathbf{n}(\mathbf{r})\right]^2, \qquad (2)$$

1

which corresponds to the usual one-constant (K) approximation of the Frank elasticity [22,18]. The anisotropic homeotropic anchoring surface energy is accounted for by the surface Hamiltonian

$$\mathcal{H}_s = \frac{1}{2} \iint d^2 \mathbf{r}_\perp \left(\delta \mathbf{n}^- \cdot \mathbf{W}^- \cdot \delta \mathbf{n}^- + \delta \mathbf{n}^+ \cdot \mathbf{W}^+ \cdot \delta \mathbf{n}^+ \right),$$

(3)

where $\delta \mathbf{n}^-(\mathbf{r}_\perp) = \delta \mathbf{n}(\mathbf{r}_\perp, 0)$ and $\delta \mathbf{n}^+(\mathbf{r}_\perp) = \delta \mathbf{n}(\mathbf{r}_\perp, d)$, and $\mathbf{W}^-$ and $\mathbf{W}^+$ are positive definite constant tensors that entail the anisotropy of the surfaces and their relative orientation. We assume that the two surfaces are identical in nature and we define $\mathbf{W}^- = W_{\max} \hat{\mathbf{x}}^- \otimes \hat{\mathbf{x}}^- + W_{\min} \hat{\mathbf{y}}^- \otimes \hat{\mathbf{y}}^-$ and $\mathbf{W}^+ = W_{\max} \hat{\mathbf{x}}^+ \otimes \hat{\mathbf{x}}^+ + W_{\min} \hat{\mathbf{y}}^+ \otimes \hat{\mathbf{y}}^+$, where $\hat{\mathbf{x}}^\pm$ and $\hat{\mathbf{y}}^\pm$ denote the hard and weak axis on plate $\pm$, respectively (see Fig. 1). The eigenvalues $W_{\max}$ and $W_{\min}$ naturally define two extrapolation lengths $\lambda_{\min} = K/W_{\max}$ and $\lambda_{\max} = K/W_{\min}$ [18]. We assume extreme anisotropy, namely $\lambda_{\min} \ll \lambda_{\max}$.
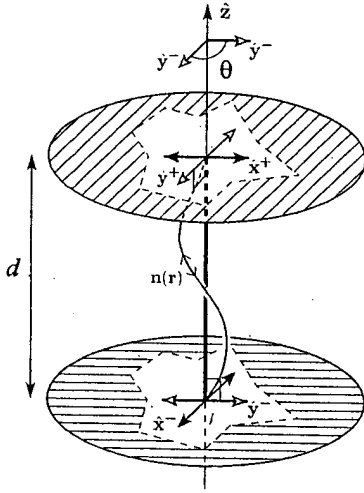

FIG. 1. Sketch of a fluctuation of the bulk director field n(r) (thin line) around its mean value $\hat{z}$ (bold line). The two anisotropic plates impose a homeotropic anchoring (i.e., the preferred surface value of n is $\hat{z}$) characterized by an anisotropic anchoring elasticity: deviations from $\hat{z}$ are easier in the "soft" directions $\hat{\mathbf{y}}^\pm$ than in the "hard" directions $\hat{\mathbf{x}}^\pm$. In this geometry, the fluctuation-induced "Casimir" interaction between the plates depends both on their separation d and their relative angle θ.

"Casimir" effects arise from the quantization of the fluctuation modes by the boundaries (essentially from the suppression of modes of wavevector smaller than $2\pi/d$). The actual effect of the boundaries on a fluctuation mode of wavevector $q \simeq 2\pi/d$ is a function of the product $q\lambda$, where λ is the extrapolation length corresponding to the considered polarization of the fluctuation. Depending on the relative values of $\lambda_{\min}$, $\lambda_{\max}$ and d, three different regimes occur: (i) For $\lambda_{\min} \ll \lambda_{\max} \ll d$ the constraints are effectively hard in both directions and the anisotropy is washed out at leading order. (ii) For $\lambda_{\min} \ll d \ll \lambda_{\max}$ the director field is subject to a hard constraint in the x direction while it is virtually free in the (perpendicular) y direction. (iii) Finally, for $d \ll \lambda_{\min} \ll \lambda_{\max}$ both directions allows almost free fluctuations and the anisotropy is lost again at leading order. To emphasize the effect of the anisotropy, we thus focus on the case where $\lambda_{\min} \ll d \ll \lambda_{\max}$.

Following Ref. [7], we now proceed to calculate the partition function for the director fluctuations, using $\mathcal{H} + \mathcal{H}_s$ as the total Hamiltonian. The quantum mechanical description of the partition function [7], which treats z as an imaginary time variable, helps us gain a useful insight into the meaning of the boundary conditions. From the "imaginary time action" $\mathcal{H}$, one can define the "momentum" conjugate to a component of $\delta \mathbf{n}$ as $P_{\delta n} = K \partial_z \delta n$. Then, one can go from coordinate space to momentum space. In particular, at the boundaries one finds out that $P_{\delta n}$ is quadratically confined by the tensor $\mathbf{W}^{-1}$ and thus acts opposite as compared to δn. In other words, there is an uncertainty principle relating the fluctuations of δn and $\partial_z \delta n$ as $\Delta(\delta n)\Delta(\partial_z \delta n) \simeq k_B T/K$. In light of this, one can argue that the boundary condition of nearly free fluctuations in the soft direction is asymptotically equivalent to setting $\partial_z \delta n = 0$. Note that this is equivalent to assuming that the directors cannot bear torques due to the freedom of rotation in the soft direction.

With the above justification, we can employ a somewhat less involved path integral formulation [1,6] using the following boundary conditions: $\delta \mathbf{n}^\pm \cdot \hat{\mathbf{x}}^\pm = 0$, $\partial_z \delta \mathbf{n}^\pm \cdot \hat{\mathbf{y}}^\pm = 0$. The partition function of the fluctuating director field subject to the above constraints can be written as

$$\mathcal{Z} = \int \mathcal{D}\delta \mathbf{n}(\mathbf{r}) \; \delta\{\delta \mathbf{n}^- \cdot \hat{\mathbf{x}}^-\} \; \delta\{\partial_z \delta \mathbf{n}^- \cdot \hat{\mathbf{y}}^-\}$$

(4)

$$\times \; \delta\{\delta \mathbf{n}^+ \cdot \hat{\mathbf{x}}^+\} \; \delta\{\partial_z \delta \mathbf{n}^+ \cdot \hat{\mathbf{x}}^+\} \; e^{-\mathcal{H}/k_B T}.$$

The functional delta functions can be written as integral representations by introducing four Lagrange multiplier surface fields:

$$\mathcal{Z} = \int \mathcal{D}\delta \mathbf{n}(\mathbf{r}) \, \mathcal{D}l_1(\mathbf{r}_\perp) \, \mathcal{D}l_2(\mathbf{r}_\perp) \, \mathcal{D}l_3(\mathbf{r}_\perp) \, \mathcal{D}l_4(\mathbf{r}_\perp) \; \exp\left\{ -\frac{\kappa}{2} \iiint d^3\mathbf{r} \, [\nabla \delta \mathbf{n}(\mathbf{r})]^2 \right.$$

(5)

$$\left. + i \iint d^2\mathbf{r}_\perp \left[l_1(\mathbf{r}_\perp) \, \delta \mathbf{n}^-(\mathbf{r}_\perp) \cdot \hat{\mathbf{x}}^- + l_2(\mathbf{r}_\perp) \, \partial_z \delta \mathbf{n}^-(\mathbf{r}_\perp) \cdot \hat{\mathbf{y}}^- + l_3(\mathbf{r}_\perp) \, \delta \mathbf{n}^+(\mathbf{r}_\perp) \cdot \hat{\mathbf{x}}^+ + l_4(\mathbf{r}_\perp) \, \partial_z \delta \mathbf{n}^+(\mathbf{r}_\perp) \cdot \hat{\mathbf{y}}^+ \right] \right\},$$

where $\kappa = K/k_B T$. The integration over the director field is now Gaussian and can be easily performed. It yields

$$\mathcal{Z} = \int \mathcal{D}l_1(\mathbf{q}_\perp)\,\mathcal{D}l_2(\mathbf{q}_\perp)\,\mathcal{D}l_3(\mathbf{q}_\perp)\,\mathcal{D}l_4(\mathbf{q}_\perp)\,\exp\left\{-\frac{1}{4\kappa}\sum_{\alpha,\beta=1}^{4}\iint\frac{d^2\mathbf{q}_\perp}{(2\pi)^2}\,l_\alpha(-\mathbf{q}_\perp)\,M_{\alpha\beta}(\mathbf{q}_\perp)\,l_\beta(\mathbf{q}_\perp)\right\},\qquad (6)$$

in which

$$M(q) = \begin{bmatrix} \dfrac{1}{q} & 0 & \dfrac{e^{-qd}}{q}\cos\theta & -e^{-qd}\sin\theta \\[2ex] 0 & -q & e^{-qd}\sin\theta & -qe^{-qd}\cos\theta \\[2ex] \dfrac{e^{-qd}}{q}\cos\theta & e^{-qd}\sin\theta & \dfrac{1}{q} & 0 \\[2ex] -e^{-qd}\sin\theta & -qe^{-qd}\cos\theta & 0 & -q \end{bmatrix}, \qquad (7)$$

where θ is the angle between the corresponding soft axes of the two plates (see Fig. 1). The remaining integration over the Lagrange multiplier fields can be performed to give $\ln\mathcal{Z} = -\frac{1}{2}\sum_{\mathbf{q}_\perp}\ln\left(\det M(\mathbf{q}_\perp)\right)$, which leads to a simple expression for the free energy per unit area:

$$\mathcal{F}(\theta, d) = \frac{k_\mathrm{B}T}{2\pi d^2}\int_0^\infty du\, u\, \ln\left[1 - e^{-2u}\cos 2\theta\right]. \qquad (8)$$

Integration over u then gives the final result Eq. (1) above. The function $f(\theta) = \sum_{k=1}^{\infty}\cos^k(2\theta)/k^3$ which describes the orientational dependence of the interaction has the structure of a zeta function that is commonly present in "Casimir" interactions.

It is instructive to examine the limiting cases of plates in which the corresponding hard and soft axes are parallel or perpendicular to each other. For $\theta = 0$ the boundary conditions corresponds to a hard-hard configuration for one component of $\delta\mathbf{n}$ and a soft-soft one for the other. One can check that $f(0) = \zeta(3) \simeq 1.20206$ (ζ is the zeta function), thus we obtain exactly the same expression for the "Casimir" energy as in Ref. [7] for "alike" boundary conditions. On the other hand $f(\frac{\pi}{2}) = -\frac{3}{4}\zeta(3)$, which gives the same result as in Ref. [7] for "unlike" boundary conditions ($\theta = \pi/2$ corresponds to a soft-hard configuration for both components of $\delta\mathbf{n}$).

Our calculation suggests two kind of experiments: (i) a direct measure of the torque exerted between two plates at a fixed separation, and (ii) a measure of force as a function of separation for plates at various angles.

A possible experimental setup for the direct observation of the fluctuation-induced torque could be a torsion pendulum similar to the one discussed in Ref. [23]. Our results imply that the torsion coefficient of the pendulum k (defined as the ratio between the torque τ and the angular rotation $\Delta\theta$) is corrected at $\theta = 0$ by an amount

$$\Delta k = \frac{\pi^2}{12} \times \frac{k_\mathrm{B}TR^2}{d^2}, \qquad (9)$$

due to the "Casimir" effect. Here R is the radius of the plates of area πR^2. Using the typical values $k_\mathrm{B}T =$ 4.1×10^{-14} dyn cm, $R = 1.5$ cm, $d = 10^{-4}$ cm, one obtains $\Delta k \sim 10^{-5}$ dyn cm. This accuracy may be reachable using modern micro-manipulation techniques.

A measure of the force-distance relation for various angles θ could also be performed. An advantage of this procedure, as compared to measurement of the "simpler" effect corresponding to isotropic anchoring, is that relative effects are more easily detectable. Indeed, while the weak signal of the "Casimir" force can be swamped by stronger effects (Van der Waals, etc.), the difference between measurements performed at $\theta = 0$ and $\theta = 90°$ should provide a differential evidence of the Casimir scaling.

[1] For a review, see M. Kardar and R. Golestanian, Rev. Mod. Phys. 71, 1233 (1999).
[2] M. Krech, The Casimir Effect in Critical Systems (World Scientific, Singapore, 1994).
[3] V. M. Mostepanenko and N.N. Trunov, The Casimir Effect and Its Applications (Clarendon Press, Oxford, 1997).
[4] H. B. G. Casimir, Proc. Kon. Ned. Akad. Wetenschap B 51, 793 (1948).
[5] K. Symanzik, Nucl. Phys. B190, 1 (1981).
[6] H. Li and M. Kardar, Phys. Rev. Lett. 67, 3275 (1991); Phys. Rev. A 46, 6490 (1992).
[7] A. Ajdari, L. Peliti, and J. Prost, Phys. Rev. Lett. 66, 1481 (1991); A. Ajdari, B. Duplantier, D. Hone, L. Peliti, and J. Prost, J. Phys. II 2, 487 (1992).
[8] D. Bartolo, D. Long and J.-B. Fournier. Europhys. Lett.

49, 729 (2000).

[9] P. Ziherl, R. Podgornik, and S. Žumer, Phys. Rev. Lett. **82**, 1189 (1999).

[10] P. Ziherl, F. K. P. Haddadan, R. Podgornik, and S. Žumer, Phys. Rev. E **61**, 5361 (2000).

[11] M. Goulian, R. Bruinsma, and P. Pincus, Europhys. Lett. **22**, 145 (1993).

[12] R. Golestanian, M. Goulian, and M. Kardar, Europhys. Lett. **33**, 241 (1996); Phys. Rev. E **54**, 6725 (1996); R. Golestanian, Phys. Rev. E, **62**, 5242 (2000).

[13] P. G. Dommersnes and J.-B. Fournier. Europhys. Lett. **46**, 256 (1999); Eur. Phys. J. B **12**, 9 (1999).

[14] F. Oosawa, *Polyelectrolytes* (Marcel Dekker, New York, 1971).

[15] J.-L. Barrat and J.-F. Joanny, Adv. Chem. Phys. **XCIV**, 1 (1996).

[16] R. Podgornik and V. A. Parsegian, Phys. Rev. Lett. **80**, 1560 (1998).

[17] B.-Y. Ha and A. J. Liu, Europhys. Lett. **846**, 624 (1999).

[18] P.-G. de Gennes and J. Prost, *The Physics of Liquid Crystals* (Clarendon, Oxford, 1993).

[19] Note that similar ideas have been recently introduced in the case of electromagnetic quantum fluctuations by O. Kenneth and S. Nussinov, preprint hep-th/9802149; hep-th/0001045.

[20] G. P. Bryan-Brown, C. V. Brown, I. C. Sage, and V. C. Hui, Nature **392**, 365 (1998).

[21] R. Barberi, private communication.

[22] F. C. Frank, Discuss. Faraday Soc. **25**, 19 (1958).

[23] S. Faetti, M. Gatti, and V. Palleschi, J. Physique Lett. **46**, L-881 (1985).

4

Molecular engineering of discotic nematic liquid crystals

SANDEEP KUMAR

Centre for Liquid Crystal Research, P.O. Box 1329, Jalahalli, Bangalore 560 013, India
Present Address: Raman Research Institute, C.V. Raman Avenue, Bangalore 560 080, India

Abstract. Connecting two columnar phase forming discotic mesogens via a short rigid spacer leads to the formation of a π-conjugated discotic dimer showing discotic nematic (N_D) phase. Attaching branched-alkyl chains directly to the core in hexaalkynylbenzene resulted in the stabilisation of N_D phase at ambient temperature. Pentalkynylbenzene derivatives possessing a combination of normal- and branched-alkoxy chains display a very broad N_D phase which is stable well below and above the room temperature.

1. Introduction

Twenty-five years have passed since the first discotic liquid crystals (LCs) have been synthesised at the Raman Research Institute in Bangalore [1]. During these two and half decades, more than 3000 discotic LCs have been prepared and characterised [2,3]. Discotic LCs constitute a vital family of functional materials with immense applications such as photoconductors, one-dimensional conductors, light emitting diodes, photovoltaic solar cells, gas sensors, etc. [4].
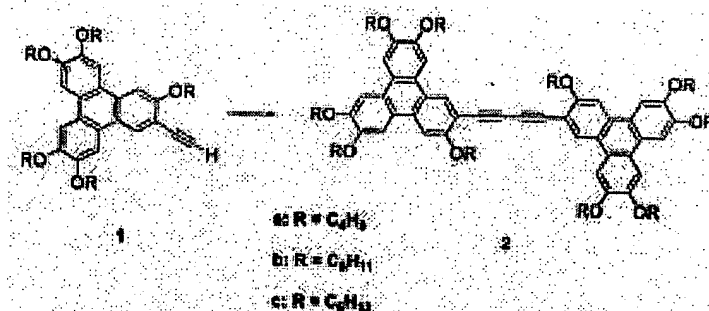
Discotic LCs are mostly composed of a π-conjugated central core substituted with usually 3 to 8 flexible aliphatic chains at its periphery. Probably because of intense π–π interactions, a majority of these materials (about 95%) form columnar mesophases and only a small number show a nematic phase. In the columnar phases molecules are stacked one on top of the other into columns and the columns posses two-dimensional long-range positional order. In the discotic nematic phase, there is only an orientational order of the discs with no long-range translational order. The negative birefringence film formed by polymerised nematic discotic LCs has been commercialised as compensation foils to enlarge the viewing angle of twisted nematic liquid crystal displays (LCDs) [5]. We have recently proposed a wide viewing liquid crystal display device based on discotic nematic LC [6].

The primary objectives of this research programme are: (a) design and synthesis of organic molecules which can form discotic nematic mesophase and (b) synthetic modifications in known discotic nematic phase forming materials to stabilise the nematic phase well below and above the room temperature.

199

2. Design and synthesis of discotic nematic liquid crystals

Molecular assembly of columnar phase forming discotic LCs with basic structural features, flat or nearly flat aromatic cores surrounded by flexible alkyl chains is often simple and a number of monomeric discotic LCs displaying columnar phases have been prepared using this technique. Discotic dimers in which two molecules are connected to each other via a long flexible alkyl chain spacer also form columnar phases as the molecules have sufficient flexibility to stack in adjacent columns [7]. Similarly, discotic oligomers and polymers are also reported to form columnar mesophases [8].

It was anticipated that linking two discotic molecules via a short rigid spacer might experience some steric hindrance due to overlapping or interdigitating aliphatic side chains and a weak distortion of the planarity of the core. This may reduce the strong π–π interactions. The rigid molecules may stay in more or less parallel position having orientational order but may lose their long range translational order and, therefore, likely to form discotic nematic phase. Compounds **2a–c** were designed to verify this idea [9]. These twins were prepared by the dimerisation of free monoacetylenes **1a–c** which in turn can be prepared from monobromopentaalkoxytriphenylenes [9].
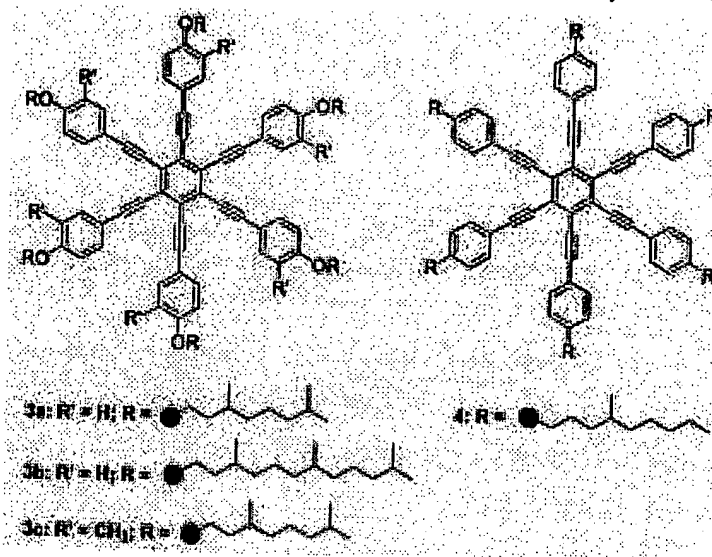

As predicted, all the dimers form discotic nematic phase over a wide temperature range. The crystalline compounds **2a**, **2b** and **2c** melt at 188.6, 161 and 135.3 °C respectively to nematic phase. The liquid crystalline phase changes to isotropic phase at 243.5, 215.9 and 172.8° respectively. Upon cooling the isotropic liquid, classical Schlieren texture was observed in all the cases. The crystallisation occurs at 172.8, 152.8 and 126.5 °C respectively in all the three materials on further cooling.

3. Design and synthesis of room-temperature discotic nematic liquid crystals

Benzene-centred multiynes are the mesogens of choice to prepare room-temperature discotic nematic liquid crystals as a number of compounds of this class are already known to show stable discotic nematic phase [2,10]. Therefore, some minor structural modifications may lead to materials having room-temperature discotic nematic phase.

The use of branched chains in liquid crystals often reduces melting and isotropic temperatures. The decrease in the transition temperature could be due to the disorder caused by branched chains and stereoheterogeneity. This methodology has been successfully applied to reduce melting and isotropic temperatures of several discotic liquid crystals forming

columnar mesophases [11]. Compounds **3a** and **3b** were designed and prepared to check if this technique is also effective in the case of alkoxymultiynes-based discotic nematic liquid crystals. Disappointingly, compound **3b** having 3,7,11-trimethyldodecane periphery was found to be non-liquid crystalline and compound **3a** with 3,7-dimethyloctane periphery showed only a high-temperature mesophase. It melts at 80°C to a nematic phase which clears at 124°C. On cooling the nematic phase appears at 123°C and crystallises at 64°C.
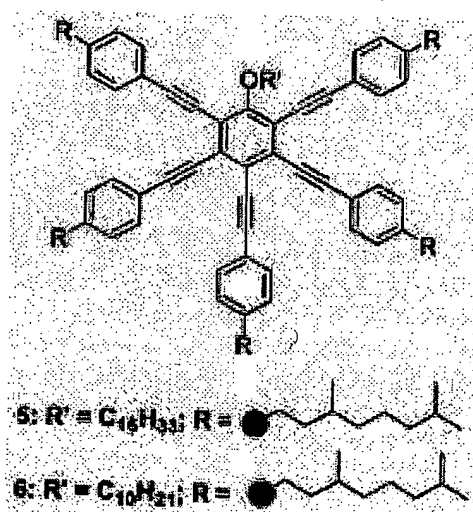

It has been observed that in the case of several triphenylene-based discotic nematic liquid crystals, a lateral methyl group substitution reduces the transition temperatures significantly [12]. Surprisingly, compound **3c** with a lateral methyl group and branched-alkoxy chain substitution does not show any such effect. In fact, the isotropic temperature increases on lateral methyl group substitution in hexaalkynylbenzene. Compound **3c** on heating exhibits a N_D phase at 71°C. Its colour changes from light yellow to brownish on heating to isotropic temperature (broad 147–160°C) indicating partial decomposition of the material at higher temperature.

From the reported thermal data of alkyl- and alkoxy-substituted hexalkynylbenzene derivatives [10], it is clear that when the peripheral alkyl chains are attached to the phenyl ring in the hexaalkynylbenzene via oxygen atom, the melting and clearing temperatures are higher compared to when the alkyl chains are directly attached to the ring. For instance, the thermal behaviour of the heptyl-substituted hexaalkynylbenzene is Cr 99°C N_D 132°C while the thermal behaviour of the heptyloxy-substituted hexaalkynylbenzene is Cr 109°C N_D 193°C I [10]. Again, as mentioned above, it is also known that when the peripheral aliphatic side chains of various cores are branched, the mesophase is widened but the type of the mesophase formed is not affected by the introduction of branching in many cases [11]. Therefore, it may be logically concluded that by replacing the normal alkyl chains by branched alkyl chains connected directly to the phenyl ring, the melting points of alkynyl-benzene derivatives may reduce and thus, stabilise the mesophase. Compound **4** designed on this basis was indeed found to exhibit a nematic phase at ambient temperature. It rep-.

resents the first example of a room-temperature discotic nematic liquid crystal [13]. The compound exhibits the N_D phase between $-12°C$ and $68°C$.

A number of pentaalkynylbenzene derivatives are known to show N_D phase [10]. In these multiynes, five positions of a benzene ring are usually substituted with phenylalkynyl moieties and the remaining one position by a normal alkoxy chain. From the thermal data of known derivatives, as expected, it can be seen that increasing the length of normal alkoxy chain, decreases the melting and isotropic temperatures. An interesting example in this series is compound **5** which shows a phase transition $Tg - 36°C$ N_D $23°C$ I [10]. It is expected that shortening the *n*-hexadecyl chain would increase the isotropic temperature and thus stabilise the N_D phase at room temperature. Accordingly, compound **6** was designed and prepared. The synthesis involves alkylation of pentabromophenol with decylbromide followed by the five-fold condensation of branched-alkoxy chain-substituted phenylacetylene using Sonogashira reaction conditions. The compound was found to be discotic nematic at room temperature. Its differential scanning calorimetry exhibits a glass transition at about $-35°C$ and the isotropic temperature at $40°C$.

4. Conclusion

It has been shown that the less common discotic nematic phase can be created by a careful synthetic design. Discotic dimers in which two columnar phase forming molecules were connected to each other via a short rigid spacer exhibit discotic nematic phase. The discotic nematic phase of hexa- and penta-alkynylbenzenes can be stabilised well below and above the room temperature either by attaching branched-alkyl chain directly to the phenyl ring or by a combination of normal and branched-alkoxy chains substitution. These materials may be useful for wide viewing LCD devices.

Acknowledgement

I am grateful to Professor B K Sadashiva for helpful discussions.

References

[1] S Chandrasekhar, B K Sadashiva and K A Suresh, *Pramana – J. Phys.* **9**, 471 (1977)

[2] A N Cammidge and R J Bushby, in *Handbook of liquid crystals* edited by D Demus, J Goodby, G W Gray, H-W Spiess and V Vill (Wiley-VCH, 1998) vol. 2B, ch. VII

[3] K Praefcke, *International conference on discotic liquid crystals* (Trieste, Italy, November 25–29, 2002)

[4] N Boden and B Movaghar, in *Handbook of liquid crystals* edited by D Demus, J Goodby, G W Gray, H-W Spiess and V Vill (Wiley-VCH, 1998) vol. 2B, ch. IX

S Chandrasekhar and S Kumar, *Science Spectra* **8**, 66 (1997)

V S K Balagurusamy, S K Prasad, S Chandrasekhar, S Kumar, M Manickam and C V Yelamaggad, *Pramana – J. Phys.* **53**, 3 (1999)

D Adam, P Schuhmacher, J Simmerer, L Häussling, K Siemensmeyer, K H Etzbach, H Ringsdorf and D Haarer, *Nature* **371**, 141 (1994)

J Simmerer, B Glusen, W Paulus, A Kettner, P Schuhmacher, D Adam, K H Etzbach, K Siemensmeyer, J H Wendorff, H Ringsdorf and D Häarer, *Adv. Mater.* **8**, 815 (1996)

I H Stapff, V Stumpflen, J H Wendorff, D B Spohn and D Mobius, *Liq. Cryst.* **23**, 613 (1997)

S Marguet, D Markovitsi, P Millie, H Sigal and S Kumar, *J. Phys. Chem.* **B102**, 4697 (1998)

L Schmidt-Mende, A Fechtenkotter, K Mullen, E Moons, R H Friend and J D Mackenzie, *Science* **293**, 1119 (2001)

D Markovitsi, S Marguet, J Bondkowski and S Kumar, *J. Phys. Chem.* **B105**, 1299 (2001)

I Seguy, P Destruel and H Bock, *Synth. Met.* **111–112**, 15 (2000)

[5] H Mori, Y Itoh, Y Nishuira, T Nakamura, Y Shinagawa, *Jpn. J. Appl. Phys.* **36**, 143 (1997)

K Kawata, *The chemical record* **2**, 59 (2002)

[6] S Chandrasekhar, S Krishna Prasad, G G Nair, D S Shankar Rao, S Kumar and M Manickam, *EuroDisplay '99, The 19th International Display Research Conference Late-News Papers* (Berlin, Germany, 1999) p. 9

[7] C P Lillya and Y L N Murthy, *Mol. Cryst. Liq. Cryst.* **2**, 121 (1985)

S Kumar, M Manickam and H Schonherr, *Liq. Cryst.* **26**, 1567 (1999)

[8] N Boden, R J Bushby and A N Cammidge, *J. Am. Chem. Soc.* **117**, 924 (1995)

[9] S Kumar and S K Varshney, *Org. Lett.* **4**, 157 (2002)

[10] K Praefcke, in *Physical properties of liquid crystals: nematics* edited by D Dunmur, A Fukuda and G Luckhurst (INSPEC, London, 2001) p. 17

[11] P G Schouten, J F van der Pol, J W Zwikker, W Drenth and S J Picken, *Mol. Cryst. Liq. Cryst.* **195**, 291 (1991)

K Ohta, Y Morizumi, H Ema, T Fujimoto and I Yamamoto, *Mol. Cryst. Liq. Cryst.* **208**, 55 (1991)

D M Collard and C P Lillya, *J. Am. Chem. Soc.* **113**, 8577 (1991)

S Kumar, D S Shankar Rao and S K Prasad, *J. Mater. Chem.* **9**, 2751 (1999)

S Kumar, J J Naidu and D S Shankar Rao, *J. Mater. Chem.* **12**, 1335 (2002)

S Kumar and S K Varshney, *Liq. Cryst.* **28**, 161 (2001)

[12] T J Phillips, J C Jones and D G McDonnell, *Liq. Cryst.* **15**, 203 (1993)

P Hindmarsh, M J Watson, M Hird and J W Goodby, *J. Mater. Chem.* **5**, 2111 (1995)

[13] S Kumar and S K Varshney, *Angew. Chem. Int. Ed.* **39**, 3140 (2000)